INTERNATIONAL ATOMIC ENERGY AGENCY
UNITED NATIONS EDUCATIONAL, SCIENTIFIC AND CULTURAL ORGANIZATION
INTERNATIONAL CENTRE FOR THEORETICAL PHYSICS
I.C.T.P., P.O. BOX 586, 34100 TRIESTE, ITALY, CABLE: CENTRATOM TRIESTE

H4.SMR/845-14

Second Winter College on Optics

20 February - 10 March 1995

Super Resolution

C.H.F. Velzel

Philips Research Laboratories
Eindhoven, Netherlands

CHAPTER EIGHTEEN

Super-resolution in Microscopy

V.P. Tychinsky and C.H.F. Velzel

18.1. INTRODUCTION

In 1952, Toraldo di Francia proposed [1] that it must be possible to reconstruct details of an object smaller than the diffraction limit. Before that time it seemed that the well-established theories of resolution in microscopy, set up by Abbe [2] and Lord Rayleigh [3], did not permit such a reconstruction.

In recent times, resolution beyond the diffraction limit has been realized by many groups (see Section 18.3). But still many opticists find it difficult to believe that super-resolution is really possible, perhaps because this asks for a change of the pattern of thought in optical science.

With this chapter we want to promote the discussion about super-resolution by physical arguments – we leave the mathematics oriented part of the literature aside. In Section 18.2 we review the theoretical arguments for super-resolution, and in Section 18.3 we discuss a number of approaches towards its realization. But first we will go back to the classical theories of resolution; this will help us to give a definition of super-resolution useful for the classification of practical results.

As is well known, Abbe's theory of resolution in the microscope considers the images of gratings that are illuminated by monochromatic plane waves. With an aperture stop in the back focal plane of the objective, a true image of a grating object is obtained as long as at least two diffraction orders are transmitted by the stop. The smallest grating period for which this is the case is given by

$$d = \frac{\lambda}{2} \sin u \tag{18.1}$$

where λ is the wavelength of the illuminating wave and u is the angular radius of the stop. The situation is shown schematically in Figure 18.1. The same resolution limit is obtained with incoherent or focused illumination. The hidden assumption in this theory is that the field of view of the microscope is unbounded. In practice this is certainly not the case; in the next section we will see that the theory of super-resolution challenges Abbe's theory just on this point. From equation (18.1) follows that, because $\sin u$ cannot become larger than 1, the smallest detail resolvable in a microscope must have a size of half a wavelength.

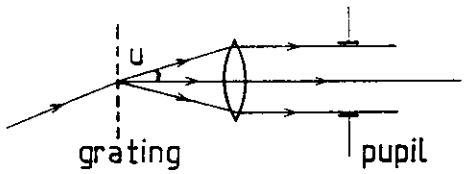

Figure 18.1 *Resolution limit according to Abbe; diffraction orders that must make an angle u with the axis are just transmitted by the aperture.*

The theory of resolution given by Lord Rayleigh considers the images of two incoherent luminous point objects. In a one-dimensional version of this theory the minimum distance at which the two can be observed separately is given also by equation (18.1). This distance is given by the width of the diffraction image of a point source. Rayleigh's theory is clearly designed for visual detection; when electronic detectors can be used it must be possible to record the intensity distribution in the image plane and process the result in such a way that the objects can be resolved at a much smaller distance. The ultimate resolution then becomes dependent on the signal-to-noise ratio of the recording.

In the rest of this chapter we cannot use either of the classical theories because we will consider mostly objects of small size (against Abbe) that are coherently illuminated (against Rayleigh). Nevertheless we will often use arguments derived from modern, extended versions of these theories, as presented for instance by Goodman [4]. It will turn out that the fact that Fourier optics, as these modern theories are called, is based on scalar wave theory is an important factor in the change of outlook suggested above.

The objects examined in recent experiments are in many cases phase objects, where the interesting details take the form of ridges, furrows or phase steps. Therefore we take, as a third form of elementary object besides gratings (Abbe) and point objects (Lord Rayleigh), the width of a ridge or in other words the distance between two phase steps as a measure of resolution. We will see in the following sections that such an object suits the theory and practice of super-resolution better than other types.

We are now ready to give our definition of super-resolution. We follow Cox and Sheppard [5] in restricting the domain of super-resolution to the observation of structures or details smaller than half a wavelength. The methods with which details down to $\lambda/2$ can be observed by microscopes with a limited numerical aperture ($\sin u < 1$) are ranged under the category of ultra-resolution. For us, super-resolution is the reconstruction of details smaller than half a wavelength, using the *a priori* knowledge* available.

In Section 18.3 we will encounter examples of ultra-resolution and super-resolution; it will be seen that by the use of the definitions given above a clear distinction can be made between the two categories.

* Some forms of *a priori* information already introduced in this section are: the object may be of finite extent, it may be a phase object, or it may have a number of discontinuities. We will see that *a priori* knowledge about the object contributes, generally speaking, to the realization of super-resolution.

18.2. THEORETICAL ARGUMENTS FOR SUPER-RESOLUTION

The possibility of ultra-resolution is built on the argument that, whereas an unlimited grating, illuminated by a plane wave (itself unlimited), leads to a far field consisting of singularities, a grating of limited extent produces a far field that is essentially non-singular. In other words: with a limited grating, illuminated by a limited wave, the diffraction orders form continuous distributions in the far field, that extend in principle to infinity in the lateral directions. An example is the Fraunhofer diffraction pattern of a slit, given by the well-known sinc distribution. In mathematical language: the Fourier transform of a function of limited support is an analytic function, and therefore can be continued over the entire frequency domain. We prefer to use physical arguments to explain ultra- and super-resolution, therefore we will not work out the mathematical reasoning [6].

We follow for a moment the description of Pask [7] and consider a one-dimensional object of length L, imaged by a lens of numerical aperture sin u (see Figure 18.2a). The far field diffraction pattern of the nth Fourier component of the object has an amplitude distribution in the form of a sine function of width $W = \lambda/L$ and with its central maximum situated at

$$\sin \alpha = n\lambda/L \tag{18.2}$$

When this central maximum lies outside the lens aperture, so that sin $\alpha >$ sin u, some of the radiation of the diffracted wave in question still reaches the image plane, where it is concentrated mainly at the edges of the geometrical image. It is difficult to extract this information from the image intensity distribution, especially in the presence of noise and other components that have their central maximum inside the lens aperture. By modulating the object field with a grating the high-frequency components can be sent through the pupil [8]; for the formation of a correct image, a demodulating grating must be applied. Figure 18.3 shows a schematic picture of a set-up, due to Lukosz, that works in this way. Because sin $\alpha < 1$ always, we only expect to obtain ultra-resolution.

The above arguments show the possibility of ultra-resolution, but not of super-resolution. However, we see already in what direction we have to go: the effective object

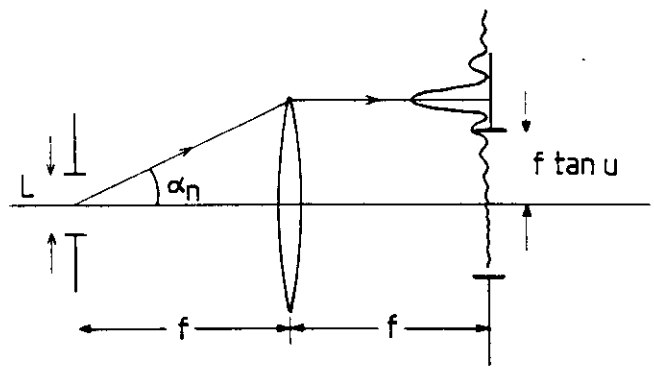

Figure 18.2 *Illustrating the transfer of information of the nth Fourier component of an object of limited extent L. The diffraction pattern in the back focal plane has its maximum outside the pupil; the boundaries of the pupil are at ± f tan u.*

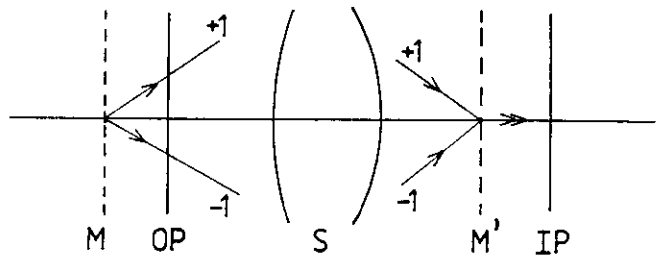

Figure 18.3 *Ultra-resolution after Lukosz [8]. The modulating grating M introduces two carrier waves +1 and −1 that are demodulated by the conjugated grating M'. OP and IP are the object and image plane.*

must be limited in extent. In the following we therefore assume that the object is illuminated by a focused beam of monochromatic light. As in practice one would use a laser for this type of illumination, we will also assume that the illuminating wave has a Gaussian intensity distribution with a width of one or several wavelengths. A different way to obtain an effective object of limited extent is given by observing the object through a small hole or through a fine grating. We will in the following consider both ways of obtaining super-resolution.

Ultra-resolution, as discussed above, can lead to reconstruction of details smaller than the diffraction limit of a given objective. Now we discuss what happens when the period of a grating object becomes smaller than the wavelength. In equation (18.2) this means that sin α should λ become larger than 1, which is impossible. Therefore no propagating diffraction orders are formed, but behind the object we find evanescent waves that carry the grating period in the transverse direction but are damped in the axial direction. With an extended object little information will reach the objective when its distance to the object is large compared to the wavelength.

When we have an (effective) object of limited extent, however, we can also break through this boundary. Bringing a small object, like a fibre tip, or a small hole in the neighbourhood of the object transforms the evanescent waves, by scattering, into propagating waves. A method of realizing super-resolution, namely scanning tunnelling, optial microscopy, will be discussed in Section 18.3.2.

Super-resolution can also be obtained with an objective placed in the far field. To make clear how this is possible, we need information carriers other than plane or evanescent waves. This was perceived by Schmidt-Weinmar [9] who introduced partial waves with a complex spatial frequency as information carries. Here we will make use of the concept of wavefront dislocations, conceived by Nye and Berry [10,11] because it suits our purpose of explaining super-resolution by physical arguments better. It should be noted that a dislocation field can be composed of complex-frequency partial waves (see reference [10], p. 267).

A dislocation in a wavefront occurs at those points where the phase of the wave is undetermined and therefore the amplitude must be zero. The contours of zero amplitude in interference patterns and speckle fields are dislocations of a special, stationary type (in the original papers of Nye and Berry most of the discussion refers to dislocations in pulsed fields). Such dislocations arise when a monochromatic wave is transmitted or reflected by an object with sharp edges or discontinuities of the refractive index.

As an illustration we consider an object with a π-jump in its phase transmission at the centre of the illuminating wave (for instance a single step of heigh $\lambda/4$ on a

reflecting object). Although we do not know the amplitude of the scattered wave in an arbitrary plane parallel to the object (in a scalar theory this would follow from e.g. a Kirchhoff integral) we know with certainty that there is a dislocation everywhere in the symmetry plane through the edge. This dislocation is also present in the far field and, when an image is made by a symmetrical instrument, the dislocation persists unto the image plane. This is even true when the imaging system has aberrations. The intensity distribution may be smeared out by diffraction, but the phase distribution displays the same π-jump as the field in the object plane (Figure 18.4). A step with a height different from π (in phase) can be decomposed in a π-jump plus a coherent background. The same treatment can then be given to the field in the neighbourhood of the axis, leading to a phase distribution in the image plane that displays a sudden change. We conclude that wavefront dislocations are carriers of information about discontinuities in the object.

In Section 18.1 we defined resolution by the smallest distance between two discontinuities that can be resolved. Let us consider the object field distribution

$$E = c^2(d^2 - x^2)e^{-x^2/w^2} \tag{18.3}$$

that has two zeros at $x = \pm d$. We take $d \ll w$, the Gaussian beamwidth. In (18.3) c^2 is an energy normalization constant. This field distribution can be considered as a linear combination of Hermite–Gauss functions of order zero and two. We know that these modal functions propagate to the far field without changing their form; it follows that the two zeros remain present in the far field. With an ideal instrument this field would be reproduced exactly in the image plane; aperture limiting and aberrations make the zeros shift and the amplitude distribution change its form, but it can be shown that the topology of the phase image remains intact [12].

An exact treatment of this problem can be given with the aid of prolate spheroidal functions, the eigenfunctions of an instrument with limited field and aperture [13]. It can be shown from (18.3) that the field intensity depends linearly on d^2 when the total energy in the object field is kept constant. This means that the resolution, normalized on w, is of the order of the inverse root of the signal-to-noise ratio,

$$\frac{d_{\min}}{w} \approx \sqrt{\frac{1}{\mathrm{SNR}}} \tag{18.4}$$

This result agrees qualitatively with a theory of Cox and Sheppard [5] that departs from the concept of degrees of freedom of an optical instrument. The number of degrees of freedom is given roughly by the product of the following factors:

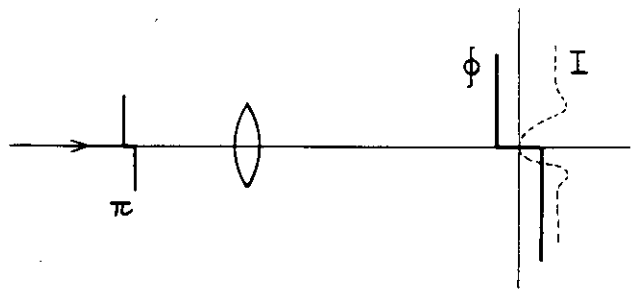

Figure 18.4 *Phase ϕ and intensity I in the image of a π-jump.*

- the space–bandwidth products in the transverse and axial space directions;
- the time–bandwidth product of the measurement;
- the dynamics of the detector (the logarithm of the signal-to-noise ratio).

These factors can be traded against each other, leaving the number of degrees of freedom invariant. Ultra-resolution means essentially the trading of field against bandwidth. Super-resolution occurs when the space–bandwidth product is brought back to 1 at the input (by masking or by focused illumination); a further increase in resolution can be obtained at the cost of signal-to-noise ratio. This is also implied by equation (18.4): the smallest details are obtained when the local intensity is decreased to noise level.

We end our discussion of the physical arguments for super-resolution by pointing out some shortcomings of the theory. Most of the papers on the theory of super-resolution do not treat the interaction of the illuminating wave with the object in great detail. We will discuss an exception in Section 3.2. Usually the scattered field is assumed to be a copy of the object; this treatment is taken over from the classical theory of microscopy. Such a model is valid when the radii of curvature in the object are large compared to the wavelength; this is the geometrical optics limit. When the details become of the order of the wavelength, or even smaller, we may expect resonance phenomena to occur, and the scattered field will depend on the orientation of the structures with respect to the polarization direction of the illuminating wave [14]. In that situation electromagnetic diffraction theory must be used to determine the effect of edges and discontinuities in the object on the topology of the scattered wave.

18.3. REALIZATIONS OF SUPER-RESOLUTION

In this section we discuss several experiments in which resolution beyond the diffraction limit was realized. As in the previous section we do not give an exhaustive (and perhaps exhausting) review of the literature, but merely discuss some recent development and assess their results.

18.3.1. Ultra-resolution by scanning confocal microscopy

Scanning confocal microscopy (SCM) satisfies one of the requirements for the realization of super-resolution in that the illuminating wave is a focused monochromatic wave (in practice a laser beam). A schematic picture of a set-up for SCM is shown in Figure 18.5. There are two different methods of detection used in practice: either a small detector is placed in the image of the source, or a detector arrangement integrates the intensity over the pupil of the objective (or parts of the pupil). The first detection method has the advantage that the axial resolution is very good, so that it can be used for making axial sections [15]. The second method does not have this property. This is because in the first method the amplitude is integrated over the pupil, in the second method the intensity. For our purpose this difference between detection methods is not relevant, the lateral resolution being equal for both. Therefore we will consider only the first detection method. The object can be scanned (in transmission or in reflection, as in Figure 18.5) by moving the beam, the microscope, or the object itself. In the

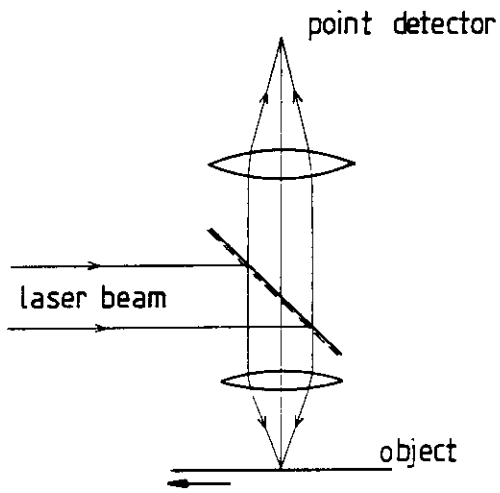

Figure 18.5 *Set-up for scanning confocal microscopy.*

arrangement of Figure 18.5 the detector signal is proportional to the square of the convolution of the object distribution with the intensity distribution of the illuminating wave. This means that the smallest detail to be resolved is given (with a square pupil) by equation (18.1) of Section 18.1.

Several ways have been found to increase the resolution in SCM beyond the classical limit. When a fluorescent object is detected by the arrangment of Figure 18.5, the object as seen by the detector signal is turned into a self-illuminator ("Selbstleuchter"). We now have an incoherent image formation situation; the intensity at the point detector is given by the convolution of the concentration distribution of the fluorescent atoms the square of the intensity distribution of the illuminating wave. Therefore the resolution is about a factor two better than that given by equation (18.1). This is a considerable gain in resolution, but it belongs according to our definition given in Section 18.1 to the category of ultra-resolution. In other variants of SCM, using a double-pass optical system and phase-conjugate mirrors [17] the resolution is also improved, but also these do not lead to super-resolution.

Next to being used as a microscopic technique, SCM has found frequent application in optical recording [18]. In that application usually pupil detection is applied, because the larger depth of focus is an advantage. Methods to improve the resolution are very interesting in optical recording, because the density of recorded information can be increased by them. We discuss some experiments in this direction.

In the scheme of Bouwhuis and Spruit [19] a layer of non-linear material is introduced just in front of the object. This layer is bleached by the illuminating beam and transmits the beam only where it is most intense. The bleached hole acts as a mask in front of the object; we have seen that this is favourable for an increase in resolution. The effect on resolution is about the same as in fluorescent SCM.

The proposal of Fukumoto [20] can be applied to magnetic optical recording only. In this experiment a triple magnetic layer is used as a recording medium. This leads to self-masking (by the upper layer) of the read-out beam so that its effective size is diminished. We have already seen that this leads to a resolution beyond the classical limit; this was confirmed by experiment.

In a recent paper by Milster and Curtis [18] several other schemes for resolution enhancement in magneto-optic recording are discussed. Although the authors use the word super-resolution in the title of their paper, most of the methods they discuss (with the exception of the scheme of Fukumoto mentioned above) do not lead to ultra-resolution, and therefore not to super-resolution either.

The conclusion of this section is that the realizations of SCM discussed lead at most to ultra-resolution, and cannot achieve super-resolution as defined in Section 18.1. In the experiments discussed no effort is made to use all the information contained in the complex amplitude distribution in the image plane. To do so more than one detector in the image plane is necessary, as we shall see in Section 18.3.3.

18.3.2. Super-resolution by scanning-tunnelling microscopy

As a second example we consider the realization of super-resolution by scanning-tunnelling optical microscopy (STOM). We have already mentioned this method in Section 18.2 and we now will discuss a few of its variants. In early versions of the method [21,22] a small diaphragm (with a diameter of the order of $\lambda/60$) was placed over the object at a very small distance (of the order of its diameter). In later work [23,24] a fine dielectric fibre tip was used to scan the object. The dimensions of the tip's radius and its distance to the object determine the resolution and image contrast. In practice a resolution of the order of $\lambda/25$ is achieved.

A schematic of the principle is given in Figure 18.6, taken from reference [23]. In this picture the illumination is provided by a plane wave totally reflected from the back side of the substrate on which the object (a transparent phase object in this case) is placed. For the study of reflecting objects it is possible to send the illuminating wave down the fibre tip [25]; the object is then locally illuminated by the light refracted and scattered by the end of the tip. It is also possible to illuminate the surface by a propagating wave [26].

Some interesting theoretical questions are connected with the research in STOM. In the past it was argued that super-resolution would violate Heisenberg's uncertainty principle, that was seen as a quantum theoretical generalization of Rayleigh's criterion. In a theoretical paper, Vigoureux and Courjon [27] show that this is not the case in STOM, because the evanescent waves used for imaging details below $\lambda/2$ have an impulse component in the object plane larger than h/λ (h is Planck's constant) so that impulse differences larger than $2h/\lambda$ can be realized and it is possible to obey the uncertainty principle while overcoming the Rayleigh limit. The fact that the lateral impulse is larger than h/λ makes the vertical impulse imaginary, so that the evanescent wave is damped in the direction perpendicular to the object plane. In the line of thought of

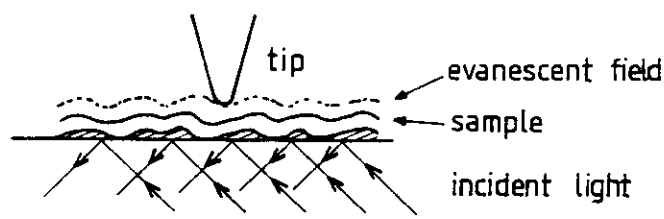

Figure 18.6 *Principle of scanning-tunnelling optical microscopy [23].*

reference [5] we could say that super-resolution is obtained by reducing the space–bandwidth product in the vertical direction.

Another problem, practical as well as theoretical, arises from the interaction of the detecting tip and the object field. The tip is polarized by the field scattered by the object; this polarization itself contributes again to the field. In reference [28] a model of this interaction is discussed; the object is represented by two small polarizable spheres and the detector by a third sphere. The radii of the three spheres and the distances between them are small compared to the wavelength of the illuminating plane wave. Using the propagator for a dipole, self-consistent equations can be set up for the electric fields at the positions of the three nanospheres. The field at the "detector" is a function of its lateral and vertical position relative to the "object". The situation is shown in Figure 18.7.

This model can explain the chief results of a STOM experiment; in order to predict the image of more complicated objects by more realistic detector bodies difficult calculations must be done. In Section 18.2 we stated that in the field of super-resolution more understanding is necessary of the interaction of electromagnetic fields and (dielectric, absorbing, metallic) submicrometre structures. This is also the case in STOM; nevertheless we can conclude that by this method super-resolution has been realized in practice.

18.3.3. Super-resolution in phase microscopy

At the end of Section 18.3.1 we concluded that by SCM ultra-resolution has been achieved, but not super-resolution; we suggested that for that purpose it would be necessary to exploit the details of the complex amplitude distribution in the image plane. Experiments in this direction have been reported by Tychinsky [12, 29, 30], who used a system consisting of a Linnik type interference microscope with focused illumination, a relay system that makes a highly magnified ($\sim 10^5 \times$) image of the focal distribution, a detector tube (image dissector) and image processing software to display the phase image in the image plane. A schematic picture of this system, called AIRYSCAN, is shown in Figure 18.8.

The objects inspected in these investigations belong to two classes: submicrometre structures on, for instance, silicon and fabricated by VLSI technology, or biological specimens on reflecting substrates. Nearly always, measured phase jumps in the image were traceable to steep edges or refractive index discontinuities in the object. The most convincing results were obtained with special semiconductor test objects with etched structures in SiO_2 layers 1–2 μm thick; slots were etched with a width of between 40 and 600 nm. The

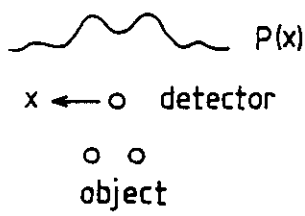

Figure 18.7 Detection of two small spheres (object by a third sphere (detector)). P(x) denotes the polarization of the detector as function of its lateral position.

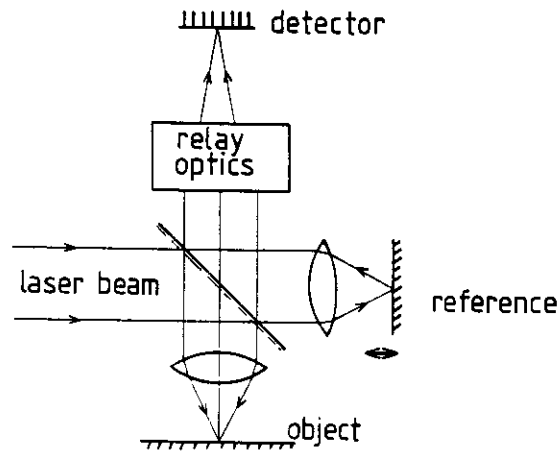

Figure 18.8 *Optics of the AIRYSCAN system. The phase of the reference beam is modulated.*

specimen structure and the measured profile of a slot of 100 nm width are shown in Figure 18.9a,b. Near the edges we see artifacts (edge ringing) in the phase image.

In all cases the measured width of the slots differed by no more than 20% from the actual size of the structure; the measured depths were, in all cases, considerably less than the actual values. For relatively large surface elements with $d>\lambda$ the topological details were exactly reproduced, but for $d<\lambda$ the profile shape and height differences depended significantly on the orientation of the E-vector of the illuminating wave.

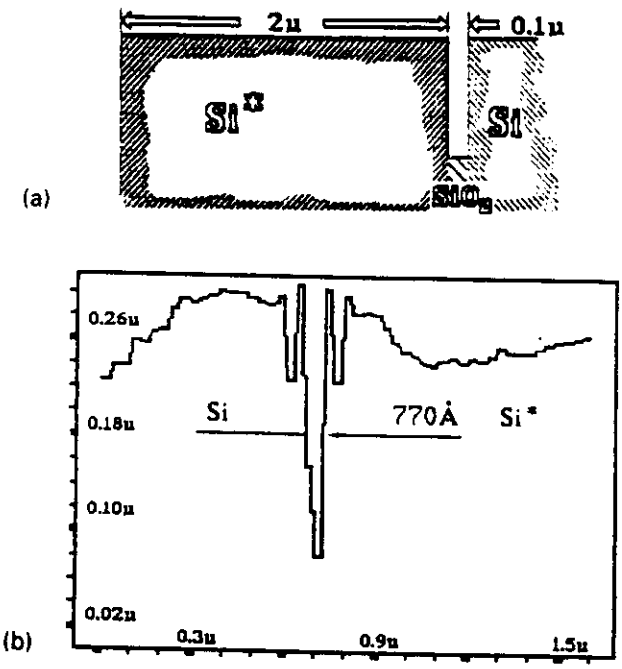

Figure 18.9 *(a) The profile of a semiconductor test object with a slit d = 0.1 μm. (b) The measured profile of the test object.*

Effective space resolution values may be also estimated from measurements of step-like objects. In reference [29] measurements were reported of growth steps on the surface of a GaAs epitaxial layer. A resolution of 5 nm was achieved, limited by the pixel size of the detector.

The recognition of phase patterns without *a priori* information is not easy due to the generic properties of phase: ambiguity, dislocations, polarization dependence, non-linearity. This is specially true for biological specimens, where also the information about thickness is obscured by refractive index gradients. In Figure 18.10 we show the complicated structure of the mycelial cell wall of Phellinus with a layer thickness of about 70 nm [30].

The possibility of the registration of dynamic processes in living cells seems to be of importance for biological research. Fourier spectra of the heartbeat of *Daphnia* were obtained at 8.65 Hz; the changes in time, under the influence of chemical stimuli, of mitochondria extracted from the mouse liver were registered.

Experiments were also performed to verify the role of wavefront dislocations in phase microscopy. In Figure 18.11a we show the phase image of a ridge, where a π-jump occurs between the points A and B which is surely absent in the surface of the specimen. A pair of conjugated screw dislocations [31] of opposite signs arises at the points A and B and the phase values on opposite sides of the cut AB belong to different Riemann surfaces. A theoretical model of such a dislocation pair is shown in Figure 18.11b. The line CD in Figure 18.11a is the boundary of a structure element of high steepness; the dislocation turns up when the height and steepness of an edge have definite values.

In this section we have shown that super-resolution can be realized by phase microscopy; the limiting resolution is determined by pixel size and noise of the detector. In images obtained by phase microscopy artefacts are observed (edge ringing, π-jumps) that have not been explained fully by the theory. A complete theory of phase microscopy,

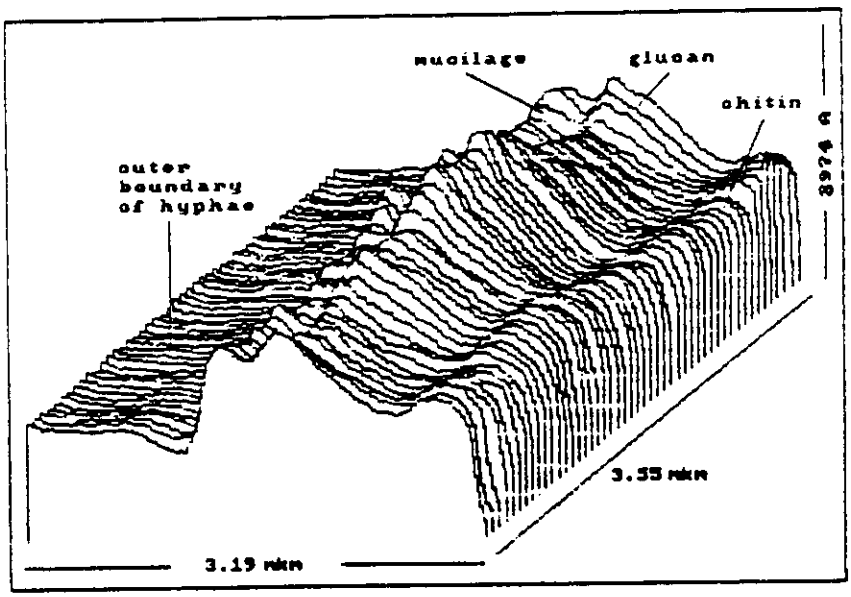

Figure 18.10 *3D image of the mycelial cell wall of* Phellinus *with structural elements of about 0.05 μm.*

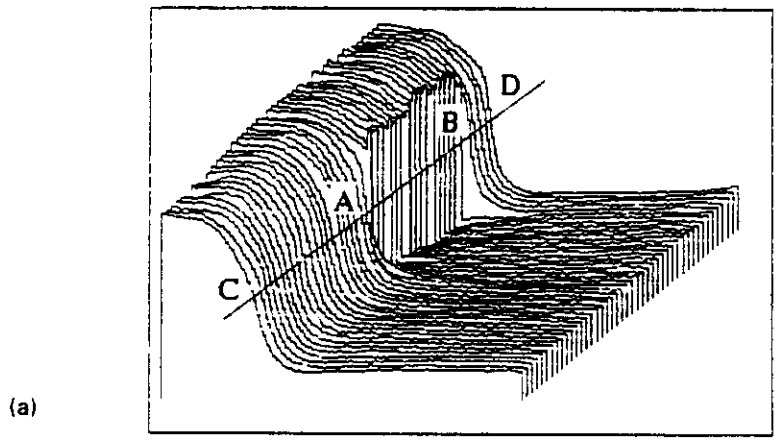

(a)

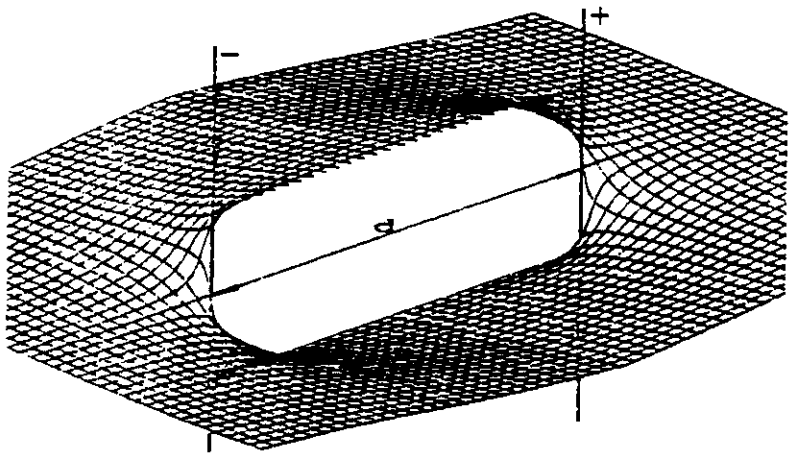

(b)

Figure 18.11 *(a) The phase image of a ridge. (b) A pair of screw dislocations.*

including the influence of the microscope (aperture, limitation, aberrations) and the interaction of the illuminating wave with the object, has not yet been given.

18.4. SUMMARY AND CONCLUSIONS

In Section 18.2 we summed up the theoretical arguments for super-resolution. We saw that the effective object size must be of the order of a wavelength; evanescent waves and wavefront dislocations are suitable carriers of information about subwavelength structure.

In Section 18.3 we discussed some experimental results. First we discussed some variants of scanning confocal microscopy (SCM); image formation in SCM can be described with the aid of plane waves as information carriers. In SCM the possibility for super-resolution exists, but in the variants we discussed only ultra-resolution (as we prefer to call it) was realized.

Super-resolution has been realized in scanning-tunnelling optical microscopy (STOM), where evanescent waves are the information carriers, and in phase microscopy, where the information is carried by wavefront dislocations.

Phase microscopy can be considered as the extension into superresolution of SCM.

We feel that the theory of super-resolution is still incomplete; the interaction of the illuminating wave with the object is not yet understood in sufficient depth and detail.

ACKNOWLEDGEMENT

This work was supported by the Russian Academy of Sciences and the Fundamental Research Foundation.

REFERENCES

1. G. Toraldo di Francia, *Nuovo Dimento*, Suppl. 3 IX, 426–438 (1952).
2. E. Abbe, *Archiv Mikrosk. Anat.* **9**, 413 (1873).
3. Lord Rayleigh, *Phil. Mag.* (5) **42**, 167 (1896).
4. J. Goodman, *Introduction to Fourier Optics*, McGraw-Hill, New York (1968).
5. I.J. Cox and C.J.R. Sheppard, *J. Opt. Soc. Am. A*, **3**, 1152–1158 (1986).
6. M. Bertero and E.R. Pike, *Optica Acta* **29**, 727–746 (1982).
7. C. Pask, *J. Opt. Soc. Am.* **66**, 68–70 (1976).
8. W. Lukosz, *J. Opt. Soc. Am.* **56**, 1463–1472 (1966); *J. Opt. Soc. Am.* **57**, 932–941 (1967).
9. H.G. Schmidt-Weinmar, in *Inverse Source Problems in Optics* (ed. H.P. Baltes), Springer, New York (1978).
10. J.F. Nye and M. Berry, *Proc. R. Soc. Lond. A* **336**, 165–190 (1974).
11. J.F. Nye, *Proc. R. Soc. Lond. A* **378**, 219–239 (1981).
12. V.P. Tychinsky, *Optics Commun.* **80**, (3,4), 1–7 (1991).
13. D. Slepian and H.O. Pollak, *Bell Syst. Tech. J.* **40**, 43 (1961).
14. J. Turunen, E. Noponen, A.H. Vasara, J.M. Miller and M. Taghizadeh *Proc. SPIE* **1718**, 90–99 (1992).
15. C.J.R. Sheppard and A. Choudhury *Optica Acta* **24**, 1051–1073 (1977).
16. J.S. Ploem, *Appl. Opt.* **26**, 3226–3231 (1987).
17. C. Mao, K.M. Johnson and W.T. Cathey, *Appl. Optics* **31**, 6272–6279 (1992).
18. T.D. Milster and C.H. Curtis, *Appl. Optics* **31**, 6272–6279 (1992).
19. G. Bouwhuis and J.H.M. Spruit, *Appl. Optics* **29**, 3766–3768 (1990).
20. A. Fukumoto and S. Yoshimura *Proc. SPIE* **1663**, 216–224 (1992)
21. E.A. Ash and G. Nicholls, *Nature* **237**, 510–512 (1972).
22. D.W. Pohl, W. Denk and M. Lanz, *Appl. Phys. Lett.* **44**, 651–653 (1984).
23. R.C. Reddick, R.J. Warmack and T.L. Ferrell, *Phys. Rev. B.* **39**, 767–770 (1989).
24. D. Courjon, K. Sarayeddine and M. Spajer, Opt. Commun. **71**, 23–28 (1989).
25. C. Girard and M. Spajer, Appl. Optics **31**, 3726–3733 (1900).
26. J.M. Vigoureux, C. Girard and D. Courjon, *Optics Lett.* **14**, 1039–1041 (1989).
27. J.M. Vigoureux and D. Courjon, *Appl. Optics* **31**, 3170–3177 (1992).
28. J.M. Vigoureux, F. Depasse and C. Girard, *Appl. Optics* **31**, 3036–3045 (1992).
29. V.P. Tychinsky, *Optics Comm.* **74**, n. 1,2, 41–45 (1989).

30. V.P. Tychinsky, A.V. Tavrov, D.O. Shepelsky and A.G. Shuchkin, *Pisma GTPH* **17**, 80–84 (1991).
31. V. Yu. Bazhenov, M.S. Soskin and M.V. Vasnetsov. *J. Mod. Optics* **39**, 985–990 (1992).